Title
Design, Synthesis, and Structure−Activity Relationships of Alkylcarbamic Acid Aryl Esters, a New Class of Fatty Acid Amide Hydrolase Inhibitors

Journal
Journal of Medicinal Chemistry, 46(12)

ISSN
0022-2623

Authors
Tarzia, Giorgio
Duranti, Andrea
Tontini, Andrea
et al.

Publication Date
2003-06-01

DOI
10.1021/jm021119g

Design, Synthesis, and Structure−Activity Relationships of Alkylcarbamic Acid Aryl Esters, a New Class of Fatty Acid Amide Hydrolase Inhibitors

Giorgio Tarzia,[†] Andrea Duranti,[†] Andrea Tontini,[†] Giovanni Piersanti,[†] Marco Mor,*[,‡] Silvia Rivara,[‡] Pier Vincenzo Plazzi,[‡] Chris Park,[§] Satish Kathuria,[§] and Daniele Piomelli[§]

Istituto di Chimica Farmaceutica e Tossicologica, Università degli Studi di Urbino Carlo Bo, Piazza del Rinascimento 6, I-61029 Urbino, Italy, Dipartimento Farmaceutico, Università degli Studi di Parma, Parco Area delle Scienze 27/A, I-43100 Parma, Italy, and Department of Pharmacology, 360 MSII, University of California, Irvine, California 92697-4625

Received December 16, 2002

Fatty acid amide hydrolase (FAAH), an intracellular serine hydrolase enzyme, participates in the deactivation of fatty acid ethanolamides such as the endogenous cannabinoid anandamide, the intestinal satiety factor oleoylethanolamide, and the peripheral analgesic and anti-inflammatory factor palmitoylethanolamide. In the present study, we report on the design, synthesis, and structure−activity relationships (SAR) of a novel class of potent, selective, and systemically active inhibitors of FAAH activity, which we have recently shown to exert potent anxiolytic-like effects in rats. These compounds are characterized by a carbamic template substituted with alkyl or aryl groups at their O- and N-termini. Most compounds inhibit FAAH, but not several other serine hydrolases, with potencies that depend on the size and shape of the substituents. Initial SAR investigations suggested that the requirements for optimal potency are a lipophilic *N*-alkyl substituent (such as *n*-butyl or cyclohexyl) and a bent *O*-aryl substituent. Furthermore, the carbamic group is essential for activity. A 3D-QSAR analysis on the alkylcarbamic acid aryl esters showed that the size and shape of the *O*-aryl moiety are correlated with FAAH inhibitory potency. A CoMSIA model was constructed, indicating that whereas the steric occupation of an area corresponding to the meta position of an *O*-phenyl ring improves potency, a region of low steric tolerance on the enzyme active site exists corresponding to the para position of the same ring. The bent shape of the *O*-aryl moieties that best fit the enzyme surface closely resembles the folded conformations observed in the complexes of unsaturated fatty acids with different proteins. URB524 (*N*-cyclohexylcarbamic acid biphenyl-3-yl ester, **9g**) is the most potent compound of the series (IC_{50} = 63 nM) and was therefore selected for further optimization.

Introduction

The fatty acid ethanolamides (FAEs) constitute a newly characterized family of lipid mediators,[1] which include the endogenous cannabinoid (endocannabinoid) anandamide[2] (arachidonoylethanolamide, **1**, Figure 1), the intestinal satiety factor oleoylethanolamide[3] (OEA, **2**, Figure 1), and the peripheral analgesic and anti-inflammatory factor palmitoylethanolamide[4] (PEA, **3**, Figure 1). The FAEs are normally present in mammalian organs and tissues, where their formation is thought to be mediated through receptor-dependent cleavage of *N*-acylphosphatidylethanolamine (NAPE), a minor phospholipid component of cell membranes.[5] After formation and release from cells, polyunsaturated FAEs such as anandamide may be eliminated via a two-step process consisting of high-affinity transport into cells,[6] followed by intracellular degradation catalyzed by the serine hydrolase, fatty acid amide hydrolase (FAAH).[7] On the other hand, saturated and monounsaturated FAEs such as OEA and PEA are not substrates for transmembrane transport and their inactivation may be exclusively mediated via FAAH-catalyzed hydrolysis.[6a,8]

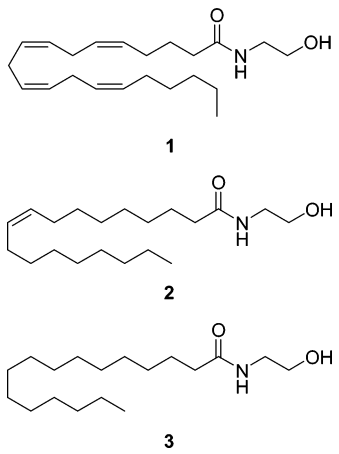

Figure 1.

Various classes of FAAH inhibitors have been identified. Reversible inhibitors include endogenous compounds such as 2-octyl-γ-bromoacetoacetate[9] (**4**, Figure 2) as well as numerous synthetic agents containing electrophilic carbonyls, such as trifluoromethyl ketones, α-keto esters, and α-keto amides.[10] Particularly promising within this group are the remarkably potent acyl heterocycles developed by Boger and collaborators,[11]

* To whom correspondence should be addressed. Phone: (0039) 0521-905063. Fax: (0039) 0521-905006. E-mail: mor@ipruniv.cce.unipr.it.
[†] Università degli Studi di Urbino Carlo Bo.
[‡] Università degli Studi di Parma.
[§] University of California.

10.1021/jm021119g CCC: $25.00
Published on Web 05/10/2003

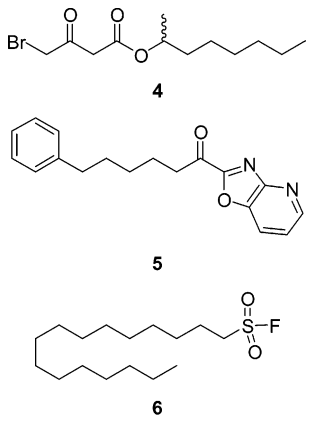

Figure 2.

among which 1-oxazolo[4,5-*b*]pyridin-2-yl ketones substituted with a C8−C12 unsaturated chain or with a phenylalkyl chain of four to eight methylene units (e.g., compound **5**, Figure 2) gave the best results. Irreversible inhibitors comprise fatty acid sulfonyl fluorides or fluorophosphonates such as hexadecanesulfonyl fluoride[12] (AM374, **6**, Figure 2).

Although the pharmacological properties of anandamide and other FAEs underscore the potential therapeutic interest of FAAH inhibition,[5b,13] the development of suitable clinical candidates from currently available inhibitors may be difficult. The presence of a lipid-like chain may confer to these compounds a number of unfavorable biopharmaceutical properties, including low water solubility, high plasma protein binding, and high accumulation in fat tissues. Furthermore, the alkyl chain also may limit the target selectivity of current FAAH inhibitors by increasing their tendency to bind to other endocannabinoid-metabolizing enzymes, such as monoglyceride lipase[14] and cannabinoid receptors.[12a,b,15] Therefore, the design of potent and selective small-molecule inhibitors of FAAH remains an essential step in the validation of this enzyme as a therapeutic target.

The cloning of rodent and human FAAH has revealed the existence of a close structural relationship among different mammalian forms of this enzyme and between these and bacterial amidases. This homology is particularly evident at the level of the amidase "signature sequence", a highly conserved domain enriched in glycine and serine residues.[7,16] Site-directed mutagenesis studies have shown that three serine residues within this domain are essential for catalytic activity (S217, S218, and S241), one of which (S241) may act as nucleophile during the catalytic process. This nucleophilic serine may be activated by the lysine residue K142 rather than through the Ser-His-Asp interaction characteristic of other serine hydrolases.[17]

In the present study, we report on the synthesis of a series of alkylcarbamic acid aryl esters (**9**), designed as inhibitors of FAAH by progressive modification of the structure of a known inhibitor of the serine hydrolase acetylcholinesterase (AChE) (compound **19**), and on the biological activity of some other known carbamates (compounds **7** and **20**−**27** in Table 1). We investigated the importance for FAAH inhibition of the carbamate group and the stereoelectronic properties of its N- and the O-substituents. In particular, we evaluated the role of the carbamate group by replacing it with isoster groups. Moreover, carbamic acid esters having confor-

Table 1. Inhibitor Potencies (IC_{50}) of Test Compounds on Fatty Acid Amide Hydrolase (FAAH) Activity

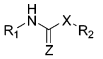

Cpds.	R_1	X	Z	R_2	IC_{50} (nM) ± S.E.M.
19	CH_3—	O	O		>30,000
20	C_2H_5—	O	O	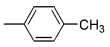	>30,000
21	CH_3—	O	O		18,290±172
22		O	O		324±31
7	*n*-C_4H_9—	O	O	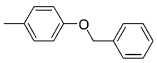	390±66
23	*n*-C_4H_9—	O	O	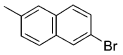	766±38
24	*n*-C_4H_9—	O	O		11,518±1,744
13		CH_2	O		>30,000
16a		NH	O		>30,000
16b		S	O		15,580±650
16c		NH	S		>30,000
16d		S	S		>30,000
18		O	S		>30,000
9a		O	O		3,776±69
9b		O	O		808±42
25		O	O	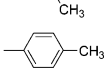	5,421±561
9c		O	O		174±31
9d		O	O	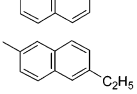	3,532±505
9e		O	O	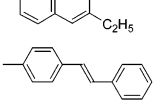	3,337±339
9f		O	O	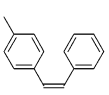	266±89
9g		O	O	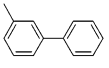	63±9
26		O	O	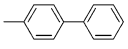	2,297±226
9h		O	O		188±36
27		O	O	—*n*-C_6H_{13}	3,755±543
9i		O	O		>30,000
11		O	O		>30,000

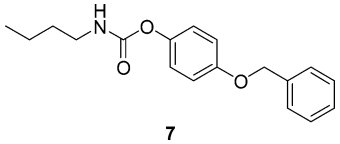

7

Figure 3.

Scheme 1[a]

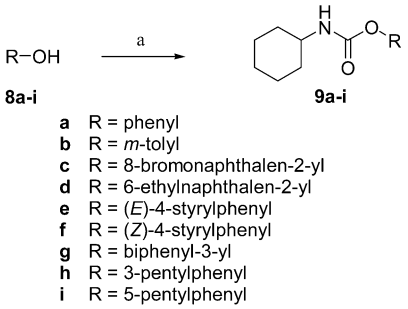

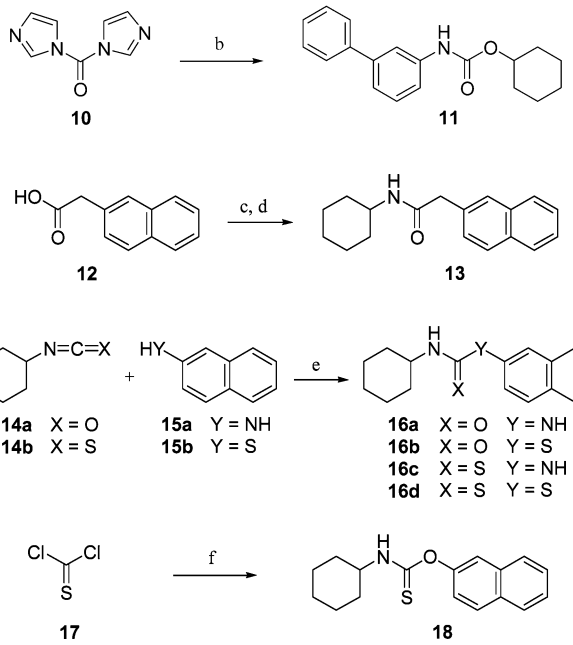

[a] Reagents and conditions: (a) *c*-$C_6H_{11}NCO$, Et_3N, toluene, reflux, 8−24 h; (b_1) biphenyl-3-ylamine, CH_3CN, DMAP, reflux, 12 h; (b_2) *c*-$C_6H_{11}OH$, reflux, 24 h; (c) $(COCl)_2$, THF, 25 °C, 2 h; (d) *c*-$C_6H_{11}NH_2$, Et_3N, CH_2Cl_2, 25 °C, 20 h; (e) Et_3N, toluene, reflux, 20 h for **16a**; *t*-BuOK, toluene, 50 °C, 15 min for **16b**; CH_2Cl_2, reflux, 14 h for **16c**; 80−100 °C, 20 h for **16d**; (f_1) sodium naphthalen-2-olate, $CHCl_3$, 25 °C, 1 h; (f_2) *c*-$C_6H_{11}NH_2$, 25 °C, 4 h.

mationally constrained *O*-aryl moieties, designed to mimic the binding conformation of the FAEs chain, allowed us to conduct a 3D-QSAR analysis of the steric requirements of the carbamate group O-substituent.

We have recently shown that representative members of this series (e.g., URB532, **7**, Figure 3) are systemically active inhibitors of FAAH activity.[18] The fact that these compounds exert profound anxiolytic-like effects in rats suggests that they may provide candidates for the development of innovative antianxiety medicines.[18]

Chemistry

The synthesis of compounds **9**, **11**, **13**, **16**, and **18** is illustrated in Scheme 1. Cyclohexylcarbamic acid aryl esters **9a**−**i** were obtained by addition of the suitable aryl alcohols to isocyanatocyclohexane. Carbamate **11** was prepared by treatment of diimidazol-1-ylmethanone (**10**) with biphenyl-3-ylamine,[19] followed by cyclohexanol, and amide **13** from naphthalene-2-carboxylic acid (**12**) via acyl chloride. The preparation of **16a**−**d** involved coupling of an iso(thio)cyanate with an appropriate thiol or amine. Finally, the thiocarbamate **18** was synthesized from thiophosgene (**17**), naphthalen-2-ol, and cyclohexylamine.

Compounds **7** and **19**−**27** were purchased from Sigma-Aldrich.

Results and Discussion

We measured FAAH activity in rat brain membranes, using [^{3}H]anandamide as a substrate.[18] Half-maximal concentrations (IC_{50}) for inhibition of FAAH activity by compounds **9a**−**i**, **11**, **13**, **16a**−**d**, and **19**−**27** are reported in Table 1. We first tested the AChE inhibitor carbaryl (**19**) and its *p*-tolyl (**20**) and 2-naphthyl (**21**) analogues. Only the latter analogue showed a weak inhibitory activity, which was enhanced by introducing more lipophilic alkyl residues on the carbamic nitrogen. Thus, replacing the methyl group of **21** with a cyclohexyl resulted in a 60-fold decrease in IC_{50} (compound **22**). Submicromolar potencies also were observed with the *n*-butyl derivatives **7** and **23**, whereas the very low activity of **24** confirmed the essential role of the O-substituent in FAAH inhibition. Importantly, unlike carbaryl (**19**), which inhibited eel acetylcholinesterase (AchE) activity with an IC_{50} of 3.1 μM, compounds **7** and **20**−**24** had no effect on the activities of this enzyme or of horse-serum butyrylcholinesterase when tested at concentrations as high as 30 μM (data not shown). Furthermore, the compounds (1−100 μM) did not displace the binding of [^{3}H]WIN-55212-2 (10 nM) to rat cerebellar CB_1 receptors or human recombinant CB_2 receptors and did not affect [^{3}H]anandamide (100 nM) transport in astrocytoma cells (data not shown).

Next, to examine the role of the carbamate function in FAAH inhibition, we prepared several isosters of **22**. Both the ester **13** and the urea **16a** were ineffective. Furthermore, replacement of oxygen with sulfur (compounds **16b**−**d**, **18**) also led to inactive analogues, with the partial exception of the thiocarbamic acid *S*-naphthyl ester **16b**. These results suggest that the carbamic group is essential for inhibition of FAAH activity by this series of compounds.

The hypothesis that guided our subsequent design was that the FAAH inhibitory activity may be improved by introducing aromatic substituents of defined shape on the oxygen atom. We further assumed that this moiety acted as a leaving group after the nucleophilic attack of the S241 residue of FAAH on the carbonyl of the inhibitors, resulting in enzyme carbamoylation. Though direct evidence for this mechanism is still needed, the findings that compound **7** inhibits FAAH activity in a noncompetitive manner (Figure 4) and that extensive dialysis (1 L/mL of sample, 16 h at 4 °C) does not reverse inhibition (data not shown) support the notion that these compounds interact irreversibly with FAAH.

Comparison of the structures of compounds **7** and **22** provided a first insight into the shape requirements for the O-substituent. A systematic conformational analysis

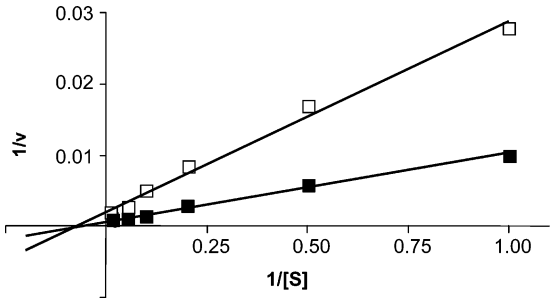

Figure 4. Lineweaver−Burke analysis of the hydrolysis of [^{3}H]anandamide (1−100 μM) by rat brain membranes in the absence (■) or presence (□) of compound **7** (1 μM). Results are from one experiment, representative of five in which maximal velocities (V_{max}) for [^{3}H]anandamide hydrolysis were 2271 ± 477 pmol/(min·mg) protein in control samples and 703 ± 188 pmol/(min·mg) protein in the presence of compound **7** (p < 0.05). Michaelis−Menten constants (K_M) were 9.3 ± 2.3 μM in control samples and 10.2 ± 3.3 μM in the presence of compound **7** (p > 0.05, Student's t test; n = 5).

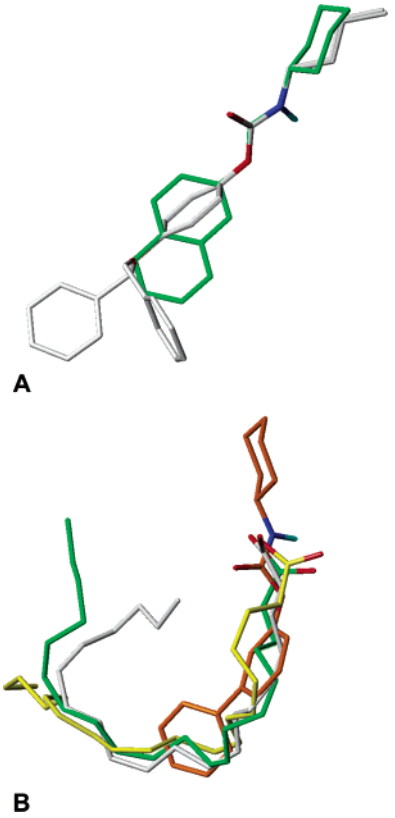

Figure 5. (A) Representation of minimum energy conformations of **22** (green carbons) and **7** (white carbons, in gauche and anti conformations) after superposition of the carbamate group. (B) Superposition of the biphenyl moiety of **9i** (orange carbons) to the lipophilic chain of arachidonic acid, cocrystallized with adipocyte lipid-binding protein (white carbons), COX-1 (yellow carbons), or COX-2 (green carbons).

of the benzyloxyphenyl fragment of **7** revealed two families of accessible conformers, mainly differing in the torsion angle around the O−CH_2 bond, with the two phenyl rings in anti or in gauche conformation. Apparently, the gauche conformation of **7** more closely resembled the shape of the naphthyl derivative **23** when the compounds were superimposed via their common carbamate group (Figure 5A). This led us to hypothesize that a bent shape of the carbamate O-substituent could favor enzyme inhibition, possibly by allowing a greater steric complementarity between the inhibitor and the active site of the enzyme. This hypothesis was further developed by supposing that the aryloxy group may mimic the fatty acid chain of anandamide and other FAEs (e.g., **1**−**3**) by counterfeiting the arrangement of the first 10−12 carbon atoms in the so-called "U-shaped" conformation of these molecules.[20]

Accordingly, we conducted a systematic exploration of the steric requirements of the aromatic O-substituents by synthesizing a series of carbamates in which the shape of the O-residue was gradually modified, while maintaining the cyclohexyl substituent on the carbamic nitrogen. Starting from the phenyl and naphthyl derivatives **9a** and **22**, we prepared a series of compounds with lipophilic groups potentially able to occupy either a region of space antipodal to the carbamate group (**9e**, **25**, **26**) or a region corresponding to the meta position of the phenyl ring (**9a**−**d**,**f**,**g**). The design of these compounds took into consideration the possibility of calculating a 3D-QSAR model correlating steric parameters with inhibitory potency after superposition of their modeled structures.

Within this second set of compounds, greater inhibitory potencies were obtained with those molecules that had a bent shape. In particular, we observed the strongest FAAH inhibition with the *m*-biphenyl derivative URB524 (**9g**), whose IC_{50} value (63 nM) indicates a 36-fold increase in potency over the isomeric *p*-biphenyl derivative **26**. The comparison between **9e** and **9f**, **9c** and **9d**, and **9b** and **25** is also suggestive of a similar trend. While the *O*-phenyl derivative **9a** was almost inactive, we obtained compounds of moderate to good inhibitory potency by substituting the meta position of **9a** with groups of suitable sizes (**9b**,**h**,**g**). Importantly, the carbamates **9a**−**g**, **25**, and **26** did not significantly interact with AChE or with cannabinoid-related targets such as CB_1 or CB_2 cannabinoid receptors and endocannabinoid transporter at concentrations as high as 30 μM.

It is noteworthy that the *m*-biphenyl fragment of **9g** may be superposed to the first 10 carbons of the fatty acid chain of arachidonic acid in the conformations adopted by this compound when bound to various proteins. The coordinates of such complexes are available through the Protein Data Bank.[21] Figure 6 shows the superposition of **9g** on arachidonic acid in the conformation the latter adopts when interacting with human adipocyte lipid-binding protein,[22] COX-1,[23] and COX-2.[24] It should be noted that the two phenyl rings of **9g** can occupy regions of space corresponding to the first two cis double bonds of arachidonic acid. A folded conformation similar to that illustrated in Figure 5B was found, together with other more straight conformations, for arachidonic acid in complex with human serum albumin.[25] Similar folded conformations also were observed for oleic acid and other unsaturated fatty acids bound to human fatty acid binding proteins (FABP).[26] These observations led us to consider the *m*-biphenyl fragment as a putative bioisoster of the first moiety of such chains, being able to reproduce the bent shape of the first two *cis*-double bonds of the arachidonyl chain.

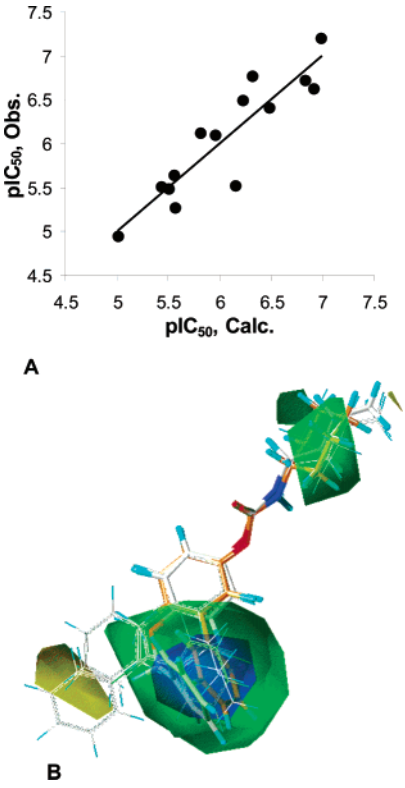

Figure 6. (A) Plot of the experimentally observed pIC_{50} data vs those calculated by the 3D-QSAR CoMSIA model for the 14 compounds reported in Table 2. A PLS model with two latent variables gave the following statistics: $r^2 = 0.82$, $s = 0.32$, $q^2_{LOO} = 0.54$. (B) 3D-QSAR graphical depiction of the coefficients for the CoMSIA fields, calculated by PLS analysis on the pIC_{50} values of the 14 compounds reported in Table 2. All the compounds are represented as lines except **7** (white carbons) and **9g** (orange carbons), which are represented as sticks. The colored volumes indicate the points where the influence of the steric potential on pIC_{50} is more significant. The color codes are the following: blue, very positive; green, positive; yellow, negative (see Experimental Section).

We next replaced the aromatic O-substituent with flexible alkyl chains. In the 2-acyloxazolopyridine series of competitive FAAH inhibitors described by Boger and collaborators,[11] the introduction of an *ω*-phenylpentyl group leads to one of the most potent inhibitors. By contrast, in our series the presence of the same moiety was detrimental to the inhibitory activity (see compounds **27** and **9i**). Together with their differences in inhibition kinetics, these results support the notion that the two classes of compounds inhibit FAAH through separate mechanisms.

A further indication of the distinct SAR profile of the *N*-alkylcarbamic acid aromatic esters described here is the fact that compound **11**, which has a bent shape like **9g** but inverted N- and O-substituents, was inactive. This suggests that the binding pockets of the two moieties have specific stereoelectronic requirements.

The correlation between molecular shape and FAAH inhibitor potency was tested by 3D-QSAR methods. A number of key compounds characterized by variations of their steric (and not electrostatic or lipophilic) features were selected, and only the correlation between steric field and biological activity was investigated. A 3D-QSAR analysis was performed by partial least squares (PLS) regression on the comparative molecular similarity index analysis (CoMSIA) steric field[27] employing, as the dependent variable, the inhibitory potency expressed on a −log scale (pIC_{50}). Only the carbamate derivatives having a lipophilic N-substituent and an aromatic O-substituent were included in the analysis, since they represented a chemically homogeneous set with an initial standard deviation in pIC_{50} values of 0.67 units around a mean value of 6.06.

Table 2. Experimental and Observed pIC_{50} Values on FAAH Activity Inhibition for the *N*-Alkylcarbamate Aryl Esters Included in the 3D-QSAR Analysis

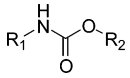

			pIC_{50}	
compd	R_1	R_2	obsd	calcd
7	*n*-butyl	benzyloxyphenyl	6.41	6.48
23	*n*-butyl	6-bromonaphthalen-2-yl	6.12	5.81
24	*n*-butyl	4-fluorophenyl	4.94	4.99
22	cyclohexyl	2-naphthyl	6.49	6.22
9a	cyclohexyl	phenyl	5.42	5.41
9b	cyclohexyl	*m*-tolyl	6.09	5.94
25	cyclohexyl	*p*-tolyl	5.27	5.55
9c	cyclohexyl	8-bromonaphthalen-2-yl	6.76	6.31
9d	cyclohexyl	6-ethylnaphthalen-2-yl	5.45	6.13
9e	cyclohexyl	(*E*)-4-styrylphenyl	5.48	5.49
9f	cyclohexyl	(*Z*)-4-styrylphenyl	6.58	6.89
9g	cyclohexyl	biphenyl-3-yl	7.20	6.98
26	cyclohexyl	biphenyl-4-yl	5.64	5.55
9h	cyclohexyl	3-pentylphenyl	6.73	6.83

The superposition of the carbamate fragments and the phenyl rings (see Experimental Section) led to a PLS model with two latent variables endowed with appreciable descriptive and predictive power ($r^2 = 0.82$, $s = 0.32$, $q^2_{LOO} = 0.54$) for the 14-compound set, whose experimental and calculated pIC_{50} values are reported in Table 2 and graphically plotted in Figure 6A.

The coefficients of the steric field are represented in Figure 8 as isopotential surfaces. As can be observed from the green and blue surfaces corresponding to a positive and very positive correlation, respectively, between steric occupancy and potency, two favorable regions were detected by our model. The first (at the top right of Figure 6B) was due to the lower mean pIC_{50} values observed for the *N*-butyl derivatives with respect to the *N*-cyclohexyl ones. It should be noted that this positive region would be much more relevant if the compounds having small N-substituents (**19**−**21**) could be included in the analysis, but this was precluded by the fact that only one of them had a measurable IC_{50}. As a consequence, the importance of the N-substituent is underestimated by our 3D-QSAR model, which, however, was developed essentially to investigate the O-substituent requirements. Indeed, a larger and deeper favorable region was observed for this moiety, as illustrated by the green and blue volumes at the bottom of Figure 6B, indicating the presence of steric bulk, positively correlated with inhibitory potency, around the meta position of the proximal ring of the *O*-biphenyl substituent. This region corresponds to the second ring of the naphthyl system (especially the areas about its 7 and 8 positions) and of the distal phenyl of the styryl substituent in its (*Z*)-configuration. It is reasonable to assume the proximity of this region to the binding site surface of FAAH, which would result in an improvement of dispersion forces and/or lipophilic interaction between

the enzyme and the inhibitor. Thus, the O-aromatic moiety, which is hypothesized to serve as a leaving group in the reaction leading to enzyme carbamoylation, would exert its effect on inhibitory potency at an early recognition stage of the process.

We observed a small region with moderately negative coefficients, represented by the yellow surface at the bottom left of Figure 6B, opposite the point of attachment of the phenyl ring to the carbamate group. It indicates that longer straight fragments can be accommodated at the binding pocket in a less efficient manner than the folded ones. The most relevant example is represented by *p*-biphenyl derivative **26**, whose potency is much lower than that of its *m*-biphenyl isomer **9g**.

We interpret the CoMSIA coefficients to indicate the existence of a large cavity with a curved shape in the active site of enzyme, where suitable O-substituents can be accommodated, so that the interaction of their carbonyl group with the active serine of the enzyme is facilitated. This result further highlights the similarity between the *m*-biphenyl moiety and the conformation of arachidonic acid bound to FABP (Figure 6), strengthening the initial hypothesis that FAEs bind to FAAH in a folded conformation, at least for the first 10 carbon atoms. We cannot exclude, however, that the fatty acyl chain of anandamide and the O-substituent of our carbamate esters are docked to different binding pockets within the FAAH active site. The availability of FAAH 3D coordinates, which were published for a covalent adduct of the enzyme with *O*-methylarachidonyl fluorophosphonate (MAFP)[28] while the present manuscript was under review, may help to resolve this issue. It is worth noting that in this crystal the arachidonyl chain of the inhibitor takes a turn after its first double bond and is flanked by aromatic residues interacting with the first two double bonds, which may be mimicked by the two phenyl rings in compound **9g**.

In conclusion, we have characterized a new class of FAAH inhibitors, namely, alkylcarbamic acid aryl esters, and demonstrated that their inhibitory potency can be improved by shape modulation of the aromatic O-substituent. The marked anxiolytic-like properties of these compounds[18] should encourage further investigations of their SAR. Indeed, a systematic structural modulation of the biphenyl derivative **9g** is currently underway in our laboratories.

Experimental Section

(a) Chemicals, Materials, and Methods. All reagents and compounds **7** and **19**−**27** were purchased from Sigma-Aldrich with the exception of **8c**,[29] **8d**,[30] **8e**,[31] **8h**,[32] and biphenyl-3-ylamine,[19] whose preparation is reported in the literature. Solvents were RP grade unless otherwise indicated. Purification of the crude materials obtained from the reactions, affording the desired products, was carried out by flash column chromatography on silica gel (Kieselgel 60, 0.040−0.063 mm, Merck). TLC analyses were performed on precoated silica gel on aluminum sheets (Kieselgel 60 F_{254}, Merck). Melting points were determined on a Büchi SMP-510 capillary melting point apparatus and are uncorrected. The structure of the unknown compounds was unambiguously assessed by MS, ^{1}H NMR, IR, and elemental analysis. EI-MS spectra (70 eV) were recorded with a Fisons Trio 1000 spectrometer. Only molecular ions (M^+) and base peaks are given. ^{1}H NMR spectra were recorded on a Bruker AC 200 spectrometer. Chemical shifts (δ scale) are reported in parts per million (ppm) relative to the central peak of the solvent. Coupling constants (J values) are given in hertz (Hz). IR spectra were obtained on a Shimadzu FT-8300 or a Nicolet Atavar spectometer. Absorbances are reported as ν (cm^{-1}). Elemental analyses were performed on a Carlo Erba analyzer. All products had satisfactory (within ±0.4 of theoretical values) C, H, N analyses results.

General Procedure for the Synthesis of Cyclohexylcarbamic Acid Aryl Esters (9a−e,g−i). To a stirred mixture of the suitable aryl alcohol **8a**−**e**,**g**−**i** (0.5 mmol) in toluene (3 mL), Et_3N (3 mg, 0.004 mL, 0.03 mmol) and *c*-$C_6H_{11}NCO$ (69 mg, 0.07 mL, 0.55 mmol) were added. After refluxing the reactants for 5 h, a further amount of *c*-$C_6H_{11}NCO$ (34 mg, 0.035 mL, 0.27 mmol) was added, and the mixture again reacted for 3 h [**9g**, 19 h; in the case of **9a**,**b** a third addition of *c*-$C_6H_{11}NCO$ (34 mg, 0.035 mL, 0.27 mmol) was necessary; overall, these reactions required 24 h; in the case of **9e**, the initial mixture was refluxed 8 h, no further addition of *c*-C_6H_{11}-NCO being necessary], then cooled, and concentrated. Purification of the residue by column cromatography (cyclohexane/EtOAc 9:1 for **9a**,**b**,**h**; 8:2 for **9i**; 85:15 for **9c**; 95:5 for **9g**; CH_2Cl_2 for **9d**,**e**) and recrystallization gave **9a**−**e**,**g**−**i**.

Cyclohexylcarbamic Acid Phenyl Ester (9a). White needles. Yield: 73% (80 mg). Mp: 137 °C (MeOH) (lit. 128−30 °C from 50% EtOH).[33] MS (EI): *m*/*z* 219 (M^+), 94 (100). ^{1}H NMR ($CDCl_3$): δ 1.20−2.05 (m, 10H), 3.57 (m, 1H), 4.91 (br s, 1H), 7.11−7.40 (m, 5H) ppm. The IR spectrum is in agreement with literature.[33] Anal. ($C_{13}H_{17}NO_2$) C, H, N.

Cyclohexylcarbamic Acid *m*-Tolyl Ester (9b). White needles. Yield: 87% (101 mg). Mp: 117−118 °C (MeOH). MS (EI): *m*/*z* 233 (M^+), 107 (100). ^{1}H NMR ($CDCl_3$): δ 1.18−2.05 (m, 10H), 2.35 (s, 3H), 3.57 (m, 1H), 4.90 (br s, 1H), 6.91−7.02 (m, 3H), 7.23 (t, 1H) ppm. IR (KBr): 3305, 1744, 1709 cm^{-1}. Anal. ($C_{14}H_{19}NO_2$) C, H, N.

Cyclohexylcarbamic Acid 8-Bromonaphthalen-2-yl Ester (9c). Yellow needles. Yield: 66% (115 mg). Mp: 170−171 °C (MeOH). MS (EI): *m*/*z* 348 (M^+), 114 (100). ^{1}H NMR ($CDCl_3$): δ 1.18−2.09 (m, 10H), 3.63 (m, 1H), 5.03 (br d, 1H), 7.26−7.99 (m, 6H) ppm. IR (KBr): 3316, 1737, 1708 cm^{-1}. Anal. ($C_{17}H_{18}BrNO_2$) C, H, N.

Cyclohexylcarbamic Acid 6-Ethylnaphthalen-2-yl Ester (9d). White needles. Yield: 74% (110 mg). Mp: 162−164 °C (MeOH). MS (EI): *m*/*z* 297 (M^+), 157 (100). ^{1}H NMR ($CDCl_3$): δ 1.17−2.07 (m, 13H), 2.81 (q, 2H), 3.61 (m, 1H), 4.97 (br d, 1H), 7.22−7.79 (m, 6H) ppm. IR ($CHCl_3$): 3440, 1732 cm^{-1}. Anal. ($C_{19}H_{23}NO_2$) C, H, N.

(*E*)-Cyclohexylcarbamic Acid 4-Styrylphenyl Ester (9e). White crystals. Yield: 86% (138 mg). Mp: 165−166 °C (MeOH). MS (EI): *m*/*z* 321 (M^+), 196 (100). ^{1}H NMR ($CDCl_3$): δ 1.22−2.05 (m, 10H), 3.56 (m, 1H), 4.91 (br d, 1H), 7.03 (d, 1H, J = 16.7), 7.12 (d, 1H, J = 16.7), 7.13 (d, 2H), 7.26−7.52 (m, 7H) ppm. IR ($CHCl_3$): 3440, 1736, 963 cm^{-1}. Anal. ($C_{21}H_{23}NO_2$) C, H, N.

Cyclohexylcarbamic Acid Biphenyl-3-yl Ester (9g). White crystals. Yield: 97% (143 mg). Mp: 141−143 °C (MeOH). MS (EI): *m*/*z* 170 (100). ^{1}H NMR ($CDCl_3$): δ 1.22−2.06 (m, 10H), 3.59 (m, 1H), 4.94 (br d, 1H), 7.12−7.61 (m, 9H) ppm. IR ($CHCl_3$): 3440, 1733 cm^{-1}. Anal. ($C_{19}H_{21}NO_2$) C, H, N.

Cyclohexylcarbamic Acid 3-Pentylphenyl Ester (9h). White crystals. Yield: 98% (142 mg). Mp: 94−95 °C (petroleum ether). MS (EI): *m*/*z* 289 (M^+), 164 (100). ^{1}H NMR ($CDCl_3$): δ 0.89 (t, 3H), 1.18−2.05 (m, 16H), 2.60 (t, 2H), 3.57 (m, 1H), 4.88 (br d, 1H), 6.93−7.27 (m, 4H) ppm. IR (KBr): 3306, 1743, 1705 cm^{-1}. Anal. ($C_{18}H_{27}NO_2$) C, H, N.

Cyclohexylcarbamic Acid 5-Phenylpentyl Ester (9i). White needles. Yield: 80% (115 mg). Mp: 55−56 °C (Et_2O/petroleum ether). MS (EI): *m*/*z* 289 (M^+), 146 (100). ^{1}H NMR ($CDCl_3$): δ 1.09−1.96 (m, 16H), 2.62 (t, 2H), 3.49 (m, 1H), 4.04 (t, 2H), 4.53 (br s, 1H), 7.16−7.28 (m, 5H) ppm. IR ($CHCl_3$): 3442, 1703 cm^{-1}. Anal. ($C_{18}H_{27}NO_2$) C, H, N.

Synthesis of (*Z*)-Cyclohexylcarbamic Acid 4-Styrylphenyl Ester (9f). A stirred mixture of benzyltriphenylphosphonium chloride (16.8 g, 43.3 mmol), 4-hydroxybenzaldehyde (5.28 g, 43.3 mmol), DBU (6.8 g, 45 mmol), and CH_3CN (67 mL) was refluxed for 4 h and concentrated. Purification of the

residue by column cromatography (cyclohexane/EtOAc 85:15) gave pure *E*-stilben-4-ol (2 g) and a 1:1 (NMR)[34] mixture of *Z*- and *E*-stilben-4-ols (0.456 g, 2.33 mmol). This was dissolved in toluene (13 mL), and Et_3N (0.014 g, 0.019 mL, 0.14 mmol) and *c*-$C_6H_{11}NCO$ (0.32 g, 0.33 mL, 2.57 mmol) were added. The mixture was refluxed under stirring for 3 h, cooled, and concentrated. Purification of the residue by column cromatography (cyclohexane/EtOAc 85:15) gave the desired product along with a substantial amount of **9e**. Recrystallization gave **9f** (105 mg) as a white solid. Mp: 131−133 °C (EtOH/H_2O). MS (EI): *m*/*z* 321 (M^+), 196 (100). ^1H NMR ($CDCl_3$): δ 1.19−2.04 (m, 10H), 3.54 (m, 1H), 4.88 (br d, 1H), 6.54 (d, 1H, J = 12.2), 6.60 (d, 1H, J = 12.2), 6.98 (d, 2H), 7.24 (m, 7H) ppm. IR ($CHCl_3$): 3440, 1736 cm^{-1}. Anal. ($C_{21}H_{23}NO_2$) C, H, N.

Synthesis of Biphenyl-3-yl Carbamic Acid Cyclohexyl Ester (11). To a stirred solution of biphenyl-3-ylamine (90 mg, 0.53 mmol) in CH_3CN (2 mL), diimidazol-1-ylmethanone (**10**) (345 mg, 2.13 mmol) and DMAP (12 mg, 0.1 mmol) were added. After the mixture was refluxed for 14 h, *c*-$C_6H_{11}OH$ (800 mg, 0.84 mL, 8 mmol) was added. The mixture reacted under reflux for 24 h and then was cooled and concentrated. Purification of the residue by column cromatography (cyclohexane/EtOAc 9:1) and recrystallization gave **11** as a white solid. Yield: 55% (86 mg). Mp: 127−129 °C (EtOH). MS (EI): *m*/*z* 295 (M^+), 141 (100). ^1H NMR ($CDCl_3$): δ 1.30−2.03 (m, 10H), 4.78 (m, 1H), 6.66 (br s, 1H), 7.31−7.47 (m, 6H), 7.59−7.70 (m, 3H) ppm. IR (KBr): 3320, 1725, 1689 cm^{-1}. Anal. ($C_{19}H_{21}NO_2$) C, H, N.

Synthesis of *N*-Cyclohexyl-2-naphthalen-2-ylacetamide (13). To a stirred, cooled (0 °C) solution of naphthalene-2-carboxylic acid (**12**) (186 mg, 1 mmol) in dry THF (3.3 mL) under N_2 atmosphere, $(COCl)_2$ (508 mg, 0.35 mL, 4 mmol) was added. The mixture was stirred at room temperature for 2 h and then concentrated. The residue was dissolved in CH_2Cl_2 (3.3 mL), and then Et_3N (283 mg, 0.39 mL, 2.8 mmol) and *c*-$C_6H_{11}NH_2$ (131 mg, 0.15 mL, 1.3 mmol) in a minimal amount of CH_2Cl_2, were added. The mixture reacted at room temperature for 20 h and then was concentrated. Purification of the residue by column cromatography (cyclohexane/EtOAc 7:3) and recrystallization gave **13** as white needles. Yield: 33% (88 mg). Mp: 185−186 °C (EtOAc). MS (EI): *m*/*z* 267 (M^+), 168 (100). ^1H NMR ($CDCl_3$): δ 0.89−1.86 (m, 10H), 3.73 (s and m, 3H), 5.26 (br s, 1H), 7.35−7.87 (m, 7H) ppm. IR (KBr): 3285, 1640 cm^{-1}. Anal. ($C_{18}H_{21}NO$) C, H, N.

Synthesis of 1-Cyclohexyl-3-naphthalen-2-ylurea (16a).[35] A stirred mixture of naphthalen-2-ylamine (**15a**) (143 mg, 1 mmol), *c*-$C_6H_{11}NCO$ (**14a**) (138 mg, 0.14 mL, 1.1 mmol), Et_3N (5 mg, 0.07 mL, 0.05 mmol), and toluene (5 mL) was refluxed for 20 h. Two further amounts of **14a** (69 mg, 0.07 mL, 0.55 mmol) were added during this period, after 5 and 3 h, respectively. The mixture was then cooled and concentrated. Purification of the residue by column chromatography (cyclohexane/EtOAc 85:15) and recrystallization gave **16a** as a white solid. Yield: 30% (80 mg). Mp: 204 °C (MeOH) (lit. 204−205 °C).[35] Anal. ($C_{17}H_{20}N_2O$) C, H, N.

Synthesis of Cyclohexylthiocarbamic Acid *S*-Naphthalen-2-yl Ester (16b).[36] To a stirred solution of *t*-BuOK (2.1 mg, 0.018 mmol) and naphthalene-2-thiol (**15b**) (300 mg, 1.875 mmol) in toluene (0.6 mL), *c*-$C_6H_{11}NCO$ (**14a**) (235 mg, 0.24 mL, 1.875 mmol) in toluene (0.6 mL) was added dropwise at 50 °C during 5 min. The mixture was stirred at the same temperature for 15 min and then cooled and filtered. Recrystallization gave **16b** as a white solid. Yield: 60% (318 mg). Mp: 153 °C (EtOH). MS (EI): *m*/*z* 159, 115 (100). ^1H NMR ($CDCl_3$): δ 0.98−1.96 (m, 10H), 3.75 (m, 1H), 5.29 (br s, 1H), 7.50−7.62 (m, 3H), 7.83−7.90 (m, 4H), 8.09 (s, 1H) ppm. IR (KBr): 3294, 1643 cm^{-1}. Anal. ($C_{17}H_{19}NOS$) C, H, N.

Synthesis of 1-Cyclohexyl-3-naphthalen-2-ylthiourea (16c). To a stirred solution of naphthalen-2-ylamine (**15a**) (143 mg, 1 mmol) in CH_2Cl_2 (2 mL), *c*-$C_6H_{11}NCS$ (**14b**) (141 mg, 0.14 mL, 1 mmol) was added. The mixture was stirred at room temperature for 5 h, refluxed for 14 h, cooled, and concentrated. Purification of the residue by column cromatography (CH_2Cl_2) and recrystallization gave **16c** as white solid. Yield: 51% (145 mg). Mp: 165−167 °C (EtOH) (lit. 172 °C from aqueous EtOH).[36] MS (EI): *m*/*z* 284 (M^+), 143 (100). ^1H NMR ($CDCl_3$): δ 1.02−2.18 (m, 11H), 4.31 (m, 1H), 6.02 (d, 1H), 7.30 (dd, 1H), 7.55 (m, 1H), 7.64 (d, 1H), 7.75−7.95 (m, 4H) ppm. IR (KBr): 3331, 3192, 1598 cm^{-1}. Anal. ($C_{17}H_{20}NS$) C, H, N.

Synthesis of Cyclohexyldithiocarbamic Acid Naphthalen-2-yl Ester (16d). A stirred mixture of naphthalene-2-thiol (**15b**) (125 mg, 0.78 mmol) and *c*-$C_6H_{11}NCS$ (**14b**) (110 mg, 0.11 mL, 0.78 mmol) was heated at 80−100 °C in a sealed tube for 20 h, cooled, and filtered. Recrystallization gave **16d** as a white solid. Yield: 46% (108 mg). Mp: 118−122 °C (toluene/*n*-pentane). MS (EI): *m*/*z* 301 (M^+), 160 (100). ^1H NMR ($CDCl_3$): δ 0.97−1.94 (m, 10H), 4.38 (m, 1H), 6.54 (br s, 1H), 7.56−7.66 (m, 3H), 7.89−8.00 (m, 3H), 8.13 (s, 1H) ppm. IR (KBr): 3337, 1580 cm^{-1}. Anal. ($C_{17}H_{19}NS_2$) C, H, N.

Synthesis of Cyclohexylthiocarbamic Acid *O*-Naphthalen-2-yl Ester (18). To a stirred solution of $C(S)Cl_2$ (**17**) (57 mg, 0.038 mL, 0.5 mmol) in $CHCl_3$ (2 mL), sodium naphthalen-2-olate [obtained as a sticky solid by adding naphthalen-2-ol (72 mg, 0.5 mmol) to a solution of Na (0.11 mg, 0.5 mmol) in dry MeOH (1 mL), stirring the mixture for 0.5 h, evaporating the solvent, and drying the residue] was added (exothermic reaction). After stirring the reactants at room temperature for 1 h, *c*-$C_6H_{11}NH_2$ (99 mg, 0.11 mL, 1 mmol) was added (exothermic reaction). The mixture reacted at room temperature for 4 h and then was concentrated. H_2O was cautiously added to the residue, and the mixture was extracted with EtOAc. The combined organic layers were dried (Na_2SO_4) and concentrated. Purification of the residue by column chromatography (cyclohexane/EtOAc 9:1) and recrystallization gave **18** as a light-yellow, garlic-smelling solid. Yield: 60% (86 mg). Mp: 154−155 °C (EtOH). MS (EI): *m*/*z* 144, 115 (100). ^1H NMR ($CDCl_3$): δ 1.22−2.22 (m, 10H), 4.14 (m, 1H), 6.64 and 6.84 (1H),[37] 7.24−7.32 (m, 1H), 7.46−7.54 (m, 3H), 7.79−7.90 (m, 3H) ppm. IR (Nujol): 3212, 1623 cm^{-1}. Anal. ($C_{17}H_{19}NOS$) C, H, N.

(b) Pharmacology. Cell fractions were prepared from brain homogenates, and membrane FAAH activity was assayed using anandamide[ethanolamine-^3H] (American Radiolabeled Chemicals, ARC (St. Louis, Missouri), 60 Ci/mmol) as a substrate.[18] [^3H]Anandamide transport assays were conducted in human astrocytoma cells, preincubating cells with inhibitors for 10 min at 37 °C, prior to exposure to [^3H]anandamide for 4 min.[8] CB_1 and CB_2 binding assays were conducted in rat cerebellar membranes (27000*g*) and CB_2-overexpressing CHO cells (purchased from Receptor Biology-Perkin-Elmer, Wellesley, MA), respectively, using [^3H]WIN-55212-2 (NEN-Dupont, Boston, MA, 40−60 Ci/mmol, 10 nM) as a ligand.[18] Cholinesterase assays were conducted with a commercial kit (Sigma, St. Louis, MO), using purified enzymes (electric eel acetylcholinesterase type V-S and horse-serum cholinesterase, both from Sigma, St. Louis, MO) and following vendor's instructions.

(c) Molecular Modeling. Molecular models were built by applying the standard tools in Sybyl, version 6.6 (Tripos Inc., 1699 South Hanley Rd, Louis, MO, 63144). Their geometries were optimized by energy minimization, employing the Merck molecular force field 94s (MMFF94s),[38] implemented in Sybyl. Conformational analysis was performed by systematic scanning of the rotatable bonds and energy minimization to a gradient of 0.01 kcal mol^{-1} $Å^{-1}$. The conformations giving the highest intersection volume with the template structure were employed for compound alignment in the following analysis. For 3D-QSAR analysis, minimum energy conformations of the compounds were aligned by a rigid root-mean-square (rms) fit of the five atoms in the carbamate fragment and the six carbon atoms in the closer phenyl ring, employing **9g** as a template structure. For compounds **7** and **9f**, the centroid of the distal phenyl ring was also superposed to that of **9g**. The CoMSIA[27] modules of Sybyl were employed for the quantitative structure−activity study. The CoMSIA steric field was calculated within a lattice with a grid resolution of 2 Å, whose extension was at least 4 Å beyond every molecular boundary in all directions. An sp^3 carbon was taken as the probe atom. Regression analyses were performed using the PLS[39] algorithm in Sybyl. The cross-validation technique with the leave-one-out (LOO)

procedure[40] was applied to calculate q^2_{LOO} as a rough estimate of the predictive power and to choose the optimal number of latent variables. Variables with an energy standard deviation lower than 2 kcal/mol were discarded to minimize the influence of noisy columns and to speed the computation. The final non-cross-validated analyses were derived with the number of latent variables corresponding to the first maximum q^2_{LOO} value, or before nonsignificant increase of q^2_{LOO} (i.e., <0.05). No filter was applied to the dependent variables in this case. The contour volumes of the 3D-QSAR model, represented in Figure 6B, correspond to the following cutoff values for the product of the PLS coefficients and the standard deviation of the steric potential: (blue) $>+0.05$, (green) $>+0.01$, (yellow) <-0.01, (red) <-0.05.

Acknowledgment. This work was supported by MIUR (Ministero dell'Istruzione, dell'Università e della Ricerca), Universities of Parma and Urbino, and the National Institute of Drug Abuse (to D.P.). The CCE (Centro di Calcolo Elettronico) and CIM (Centro Interfacoltà Misure) of the University of Parma are gratefully acknowledged for supplying the Sybyl software license.

References

(1) Fowler, C. J.; Jonsson, K.-O.; Tiger, G. Fatty acid amide hydrolase: biochemistry, pharmacology, and therapeutic possibilities for an enzyme hydrolyzing anandamide, 2-arachidonoylglycerol, palmitoylethanolamide, and oleamide. *Biochem. Pharmacol.* **2001**, *62*, 517−526 and refs 1−4 therein.

(2) Devane, W. A.; Hanuš, L.; Breuer, A.; Pertwee, R. G.; Stevenson, L. A.; Griffin, G.; Gibson, D.; Mandelbaum, A.; Etinger, A.; Mechoulam, R. Isolation and Structure of a Brain Constituent That Binds to the Cannabinoid Receptor. *Science* **1992**, *258*, 1946−1949.

(3) Rodríguez de Fonseca, F.; Navarro, M.; Gómez, R.; Escuredo, L.; Nava, F.; Fu, J.; Murillo-Rodríguez, E.; Giuffrida, A.; LoVerme, J.; Gaetani, S.; Kathuria, S.; Gall, C.; Piomelli, D. An anorexic lipid mediator regulated by feeding. *Nature (London)* **2001**, *414*, 209−212.

(4) (a) Calignano, A.; La Rana, G.; Giuffrida, A.; Piomelli, D. Control of pain initiation by endogenous cannabinoids. *Nature (London)* **1998**, *394*, 277−281. (b) Lambert, D. M.; Vandevoorde, S.; Jonsson, K.-O.; Fowler, C. J. The Palmitoylethanolamide Family: A New Class of Anti-inflammatory Agents? *Curr. Med. Chem.* **2002**, *9*, 663−674.

(5) See the following for a review. (a) Schmid, H. H.; Schmid, P. C.; Natarajan, V. The *N*-acylation−phosphodiesterase pathway and cell signaling. *Chem. Phys. Lipids* **1996**, *80*, 133−142. (b) Piomelli, D.; Giuffrida, A.; Calignano, A.; Rodríguez de Fonseca, F. The endocannabinoid system as a target for therapeutic drugs. *Trends Pharmacol. Sci.* **2000**, *21*, 218−224.

(6) (a) Di Marzo, V.; Fontana, A.; Cadas, H.; Schinelli, S.; Cimino, G.; Schwartz, J.-C.; Piomelli, D. Formation and inactivation of endogenous cannabinoid anandamide in central neurons. *Nature (London)* **1994**, *372*, 686−691. (b) Beltramo, M.; Stella, N.; Calignano, A.; Lin, S. Y.; Makriyannis, A.; Piomelli, D. Functional Role of High-Affinity Anandamide Transport, as Revealed by Selective Inhibition. *Science* **1997**, *277*, 1094−1097.

(7) See the following for a review. Deutsch, D. G.; Ueda, N.; Yamamoto, S. The fatty acid amide hydrolase (FAAH). *Prostaglandins Leukotrienes Essent. Fatty Acids* **2002**, *66*, 201−210.

(8) Piomelli, D.; Beltramo, M.; Glasnapp, S.; Lin, S. Y.; Goutopoulos, A.; Xie, X. Q.; Makriyannis, A. Structural determinants for recognition and translocation by the anandamide transporter. *Proc. Natl. Acad. Sci. U.S.A.* **1999**, *96*, 5802−5807.

(9) Patricelli, M. P.; Patterson, J. E.; Boger, D. L.; Cravatt, B. F. An Endogenous Sleep-Inducing Compound Is a Novel Competitive Inhibitor of Fatty Acid Amide Hydrolase *Bioorg. Med. Chem. Lett.* **1998**, *8*, 613−618.

(10) (a) Koutek, B.; Prestwich, G. D.; Howlett, A. C.; Chin, S. A.; Salehani, D.; Akhavan, N.; Deutsch, D. G. Inhibitors of Arachidonoyl Ethanolamide Hydrolysis. *J. Biol. Chem.* **1994**, *269*, 22937−22940. (b) Patterson, J. E.; Ollmann, I. R.; Cravatt, B. F.; Boger, D. L.; Wong, C.-H.; Lerner, R. A. Inhibition of Oleamide Hydrolase Catalyzed Hydrolysis of the Endogenous Sleep-Inducing Lipid *cis*-9-Octadecenamide. *J. Am. Chem. Soc.* **1996**, *118*, 5938−5945. (c) Boger, D. L.; Sato, H.; Lerner, A. E.; Austin, B. J.; Patterson, J. E.; Patricelli, M. P.; Cravatt, B. F. Trifluoromethyl Ketone Inhibitors of Fatty Acid Amide Hydrolase: A Probe of Structural and Conformational Features Contributing to Inhibition. *Bioorg. Med. Chem. Lett.* **1999**, *9*, 265−270.

(11) (a) Boger, D. L.; Sato, H.; Lerner, A. E.; Hedrick, M. P.; Fecik, R. A.; Miyauchi, H.; Wilkie, G. D.; Austin, B. J.; Patricelli, M. P.; Cravatt, B. F. Exceptionally potent inhibitors of fatty acid amide hydrolase: The enzyme responsible for degradation of endogenous oleamide and anandamide. *Proc. Natl. Acad. Sci. U.S.A.* **2000**, *97*, 5044−5049. (b) Boger, D. L.; Miyauchi, H.; Hedrick, M. P. α-Keto Heterocycle Inhibitors of Fatty Acid Amide Hydrolase: Carbonyl Group Modification and α-Substitution. *Bioorg. Med. Chem. Lett.* **2001**, *11*, 1517−1520.

(12) (a) Deutsch, D. G.; Lin, S.; Hill, W. A. G.; Morse, K. L.; Salehani, D.; Arreaza, G.; Omeir, R. L.; Makriyannis, A. Fatty Acid Sulphonyl Fluorides Inhibit Anandamide Metabolism and Bind to the Cannabinoid Receptor. *Biochem. Biophys. Res. Commun.* **1997**, *231*, 217−221. (b) Deutsch, D. G.; Omeir, R.; Arreaza, G.; Salehani, D.; Prestwich, G. D.; Huang, Z.; Howlett, A. Methyl Arachidonyl Fluorophosphonate: A Potent Irreversible Inhibitor of Anandamide Amidase. *Biochem. Pharmacol.* **1997**, *53*, 255−260. (c) De Petrocellis, L.; Melck, D.; Ueda, N.; Maurelli, S.; Kurahashi, Y.; Yamamoto, S.; Marino, G.; Di Marzo, V. Novel Inhibitors of Brain, Neuronal, and Basophilic Anandamide Amidohydrolase. *Biochem. Biophys. Res. Commun.* **1997**, *231*, 82−88.

(13) Bisogno, T.; De Petrocellis, L.; Di Marzo, V. Fatty Acid Amide Hydrolase, an Enzyme with Many Bioactive Substrates. Possible Therapeutic Implications. *Curr. Pharm. Des.* **2002**, *8*, 533−547.

(14) Dinh, T. P.; Carpenter, D.; Leslie, F. M.; Freund, T. F.; Katona, I.; Sensi, S. L.; Kathuria, S.; Piomelli, D. Brain monoglyceride lipase participating in endocannabinoid inactivation. *Proc. Natl. Acad. Sci. U.S.A.* **2002**, *99*, 10819−10824.

(15) (a) Fernando, S. R.; Pertwee, R. G. Evidence that methyl arachidonyl fluorophosphonate is an irreversible cannabinoid receptor antagonist. *Br. J. Pharmacol.* **1997**, *121*, 1716−1720. (b) Edgemond, W. S.; Greenberg, M. J.; McGinley, P. J.; Muthians, S.; Campbell, W. B.; Hillard, C. J. Synthesis and Characterization of Diazomethylarachidonyl Ketone: An Irreversible Inhibitor of *N*-Arachidonylethanolamide Amidohydrolase. *J. Pharmacol. Exp. Ther.* **1998**, *286*, 184−190.

(16) (a) Cravatt, B. F.; Giang, D. K.; Mayfield, S. P.; Boger, D. L.; Lerner, R. A.; Gilula, N. B. Molecular characterization of an enzyme that degrades neuromodulatory fatty-acid amides. *Nature (London)* **1996**, *384*, 83−87. (b) Kobayashi, M.; Fujiwara, Y.; Goda, M.; Komeda, H.; Shimizu, S. Identification of Active Sites in Amidase: Evolutionary Relationship between Amide Bond- and Peptide Bond-Cleaving Enzymes. *Proc. Natl. Acad. Sci. U.S.A.* **1997**, *94*, 11986−11991.

(17) (a) Patricelli, M. P.; Lovato, M. A.; Cravatt, B. F. Chemical and Mutagenic Investigations of Fatty Acid Amide Hydrolase: Evidence for a Family of Serine Hydrolases with Distinct Catalytic Properties. *Biochemistry* **1999**, *38*, 9804−9812. (b) Patricelli, M. P.; Cravatt, B. F. Clarifying the Catalytic Roles of Conserved Residues in the Amidase Signature Family. *J. Biol. Chem.* **2000**, *275*, 19177−19184.

(18) Kathuria, S.; Gaetani, S.; Fegley, D.; Valiño, F.; Duranti, A.; Tontini, A.; Mor, M.; Tarzia, G.; La Rana, G.; Calignano, A.; Giustino, A.; Tattoli, M.; Palmery, M.; Cuomo, V.; Piomelli, D. Modulation of Anxiety through Blockade of Anandamide Hydrolysis. *Nat. Med.* **2003**, *9*, 76−81.

(19) Leung, W.-Y.; Mao, F.; Haugland, R. P.; Klaubert, D. H. Lipophilic Sulfophenylcarbocyanine Dyes: Synthesis of a New Class of Fluorescent Cell Membrane Probes. *Bioorg. Med. Chem. Lett.* **1996**, *6*, 1479−1482.

(20) (a) Reggio, P. H.; Traore, H. Conformational requirements for endocannabinoid interaction with the cannabinoid receptors, the anandamide transporter and fatty acid amidohydrolase. *Chem. Phys. Lipids* **2000**, *108*, 15−35. (b) Barnett-Norris, J.; Guarnieri, F.; Hurst, D. P.; Reggio, P. H. Exploration of Biologically Relevant Conformations of Anandamide, 2-Arachidonylglycerol, and Their Analogues Using Conformational Memories. *J. Med. Chem.* **1998**, *41*, 4861−4872.

(21) Berman, H. M.; Westbrook, J.; Feng, Z.; Gilliland, G.; Bhat, T. N.; Weissig, H.; Shindyalov, I. N.; Bourne, P. E. The Protein Data Bank. *Nucleic Acids Res.* **2000**, *28*, 235−242.

(22) LaLonde, J. M.; Levenson, M. A.; Roe, J. J.; Bernlohr, D. A.; Banaszak, L. J. Adipocyte Lipid-Binding Protein Complexed with Arachidonic Acid. Titration Calorimetry and X-ray Crystallographic Studies. *J. Biol. Chem.* **1994**, *269*, 25339−25347.

(23) Malkowski, M. G.; Ginell, S. L.; Smith, W. L.; Garavito, R. M. The Productive Conformation of Arachidonic Acid Bound to Prostaglandin Synthase. *Science* **2000**, *289*, 1933−1937.

(24) Kiefer, J. R.; Pawlitz, J. L.; Moreland, K. T.; Stegeman, R. A.; Gierse, J. K.; Hood, W. F.; Stevens, A. M.; Goodwin, D. C.; Rowlinson, S. W.; Marnett, L. J.; Stallings, W. C.; Kurumbail, R. G. Structural insights into the stereochemistry of the cyclooxygenase reaction. *Nature (London)* **2000**, *405*, 97−101.

(25) Petitpas, I.; Gruene, T.; Bhattacharya, A. A.; Curry, S. Crystal Structures of Human Serum Albumin Complexed with Monounsaturated and Polyunsaturated Fatty Acids. *J. Mol. Biol.* **2001**, *314*, 955−960.
(26) Balendiran, G. K.; Schnutgen, F.; Scapin, G.; Borchers, T.; Xhong, N.; Lim, K.; Godbout, R.; Spener, F.; Sacchettini, J. C. Crystal Structure and Thermodynamic Analysis of Human Brain Fatty Acid-Binding Protein. *J. Biol. Chem.* **2000**, *275*, 27045−27054.
(27) (a) Klebe, G.; Abraham, U.; Mietzner, T. Molecular Similarity Indices in a Comparative Analysis (CoMSIA) of Drug Molecules To Correlate and Predict Their Biological Activity. *J. Med. Chem.* **1994**, *37*, 4130−4146. (b) Klebe, G.; Abraham, U. Comparative Molecular Similarity Index Analysis (CoMSIA) To Study Hydrogen-Bonding Properties and To Score Combinatorial Libraries. *J. Comput.-Aided Mol. Des.* **1999**, *13*, 1−10.
(28) Bracey, M. H.; Hanson, M. A.; Masuda, K. R.; Stevens, R. C.; Cravatt, B. F. Structural Adaptations in a Membrane Enzyme That Terminates Endocannabinoid Signaling. *Science* **2002**, *298*, 1793−1796.
(29) Snyckers, F.; Zollinger, H. Stereochemistry of the σ-Complex Intermediate in Sterically Hindered Electrophilic Aromatic Substitutions. *Helv. Chim. Acta* **1970**, *53*, 1294−1305.
(30) Buu-Hoï, Ng. Ph.; Royer, R.; Eckert, B.; Jacquignon, P. Carcinogenic Nitrogen Compounds. Part XIII.* Benzacridines, Benzocarbazoles, and Related Compounds Bearing Ethyl and Propyl Groups. *J. Chem. Soc.* **1952**, 4867−4869.
(31) Brown, B. R.; Cummings, W.; Somerfield, G. A. Polymerisation of Flavans. Part I. The Condensation of Methoxybenzyl Alcohols with Phenols. *J. Chem. Soc.* **1957**, 3757−3761.
(32) Alles, G. A.; Icke, R. N.; Feigen, G. A. Some Analogs of Synthetic Tetrahydrocannabinol. *J. Am. Chem. Soc.* **1942**, *64*, 2031−2035.
(33) Butula, I.; Čurković, Lj.; Proštenik, M. V.; Vela, V.; Zorko, F. Reactions with 1-Chlorocarbonylbenzotriazole: II. Synthesis of Carbamic Acid Esters and Related Compounds. *Synthesis* **1977**, 704−706.
(34) The signals at 7.02 (d, $J = 6.3$) and 6.84 (d, $J = 6.3$) ppm were attributed to (*E*)-stilben-4-ol. Those at 7.14 (d, $J = 8.8$) and 6.69 (d, $J = 8.8$) ppm were attributed to the (*Z*)-isomer, and the rest of the spectrum is consistent with the proposed structure.
(35) Urbański, T.; Skowrońska-Serafinowa, B.; Zylowski, J. Naphthylamidinourea and Its Reactions with Amines. *Rocz. Chem.* **1959**, *33*, 1377−1382.
(36) Brown, E. L.; Campbell, N. Studies in Qualitative Organic Analysis. Identification of Alkyl Halides, Amines and Acids. *J. Chem. Soc.* **1937**, 1699−1701.
(37) The NH proton appears to be split into two broad doublets, possibly because of tautomeric forms involving the C(S)−N bond.
(38) Halgren, T. A. Merck Molecular Force Field. I. Basis, Form, Scope, Parametrization, and Performance of MMFF94*. *J. Comput. Chem.* **1996**, *17*, 490−519.
(39) Wold, S.; Ruhe, A.; Wold, H.; Dunn, W. J. The Covariance Problem in Linear Regression. The Partial Least Squares (PLS) Approach to Generalized Inverses. *SIAM J. Sci. Stat. Comput.* **1984**, *5*, 735−743.
(40) Cramer, R. D., III.; Bunce, J. D.; Patterson, D. E. Crossvalidation, Bootstrapping, and Partial Least Squares Compared with Multiple Regression in Conventional QSAR Studies. *Quant. Struct.−Act. Relat.* **1988**, *7*, 18−25.

JM021119G